Stochastic channel model for simulation of mobile *ad hoc* networks

Gunnar Eriksson, Karina Fors, Kia Wiklundh, Ulf Sterner

Swedish Defence Research Agency (FOI), Box 1165, SE-58111 Linkoping, Sweden
E-mail: kia.wiklundh@foi.seulf.sterner@foi.se

Published in *The Journal of Engineering*; Received on 17th October 2014; Accepted on 17th October 2014

Abstract: Channel models, applicable to mobile *ad hoc* network (MANET) simulations, need to be both accurate and computationally efficient. It has been shown that inaccuracies in the channel model can seriously affect various network performance measures. It is essential that the model gives realistic time and spatial variability as the terminals move. Furthermore, the frequency selective effects from multipath propagation must be realistically modelled, so that the effects of different signalling bandwidths are captured correctly. However, to meet the necessary low-complexity constraints current commonly used channel models for network simulations are very simplified. In this study, the authors propose a model structure that is able to capture the essence of the channel characteristics, and to cope with the constraint of low computational complexity. The model describes the channel time and frequency variability between nodes in a MANET. It models the large- and small-scale fading, where the correlation between the fading parameters as well as the spatial correlation is considered. Furthermore, the study presents parameters for the proposed model based on wideband peer-to-peer channel measurements in an urban environment at 300 MHz. When analysing the link and network performance, they show that the proposed channel model describes the channel dynamics appropriately.

1 Introduction

Mobile *ad hoc* networks (MANETs) consist of mobile devices connected by wireless links. The network is characterised by peer-to-peer communication between the nodes without any centralised base station. For example, MANETs are used in vehicle communication applications and are under introduction for military use. Simulations of MANETs can be very demanding from a computational point of view. A large number of nodes, which are typical for military networks, stress the need for a channel model with low computational complexity. If we consider that the number of links between n nodes grows as $n(n-1)/2$ (assuming reciprocal channels), and that the link qualities need to be updated frequently because of mobility, the simulation time may soon get unmanageable for large networks. Hence, traditionally, very simplistic channel models – for example, two-ray models – have been used to describe the radio channel between the nodes. A summary of propagation models, used in network simulator tools, is presented in [1, Table 1]. The network performance is, however, very dependent on the dynamic behaviour of the individual links. This is a well-known problem that has been recognised by many researchers within the *ad hoc* network community, see, for example, [2–4], to give a more realistic description of the channel dynamics, the model must be able to generate both slow and fast fading; the first is mainly caused by shadowing, and the latter by that different propagation paths interfere constructively or destructively. Furthermore, the frequency selectivity of the channel (which is caused by multipath propagation) must be realistically modelled so that the effects on systems with different signal bandwidths can be investigated.

A large number of ideas have emerged on how to introduce the variability of the channels in network simulations. For example, in [5] a 'double-ring with a line-of-sight (LOS) component' model is proposed to incorporate both LOS and scattering effects for mobile scenarios. The model exhibits the statistical properties of a Rician fading channel and considers the small-scale fading for such a scenario. However, the large-scale fading and the correlation between the large-scale fading and other channel parameters are not addressed. Although the autocorrelation function of the fading envelope is derived, it is determined from the assumed theoretical model and it is not compared with real channel realisations. In [3], a different approach is adopted and the link stability and availability are modelled by using a distance transition probability matrix. The underlying channel modelling considers distance-dependent path loss, multipath and shadowing. The dynamic channel variation is generated from a semi-Markov smooth (SMS) mobility model. This link model will, to some extent, incorporate spatial correlation. However, this correlation will be determined from the SMS model and not from a certain terrain or scenario.

In recent years, there has been extensive research on the subject of channel modelling for vehicular *ad hoc* networks (VANETs). In [6], a survey of existing channel models for different scenarios in vehicular applications is presented. Several of these incorporate both small- and large-scale fading. This paper points out the key characteristics needed of channel models in VANETs and divides

Table 1 Model parameters

Description	Parameter	Value	Unit
distance dependent	n	4.15	—
	G_0	−4.8	dB
	d_{ref}	1	M
global means	$\mu_{G_{\text{LS}}}$	0	dB
	μ_K	−3.3	dB
	μ_{σ_τ}	−66.4	dBs[a]
standard deviations and corr. coeff. for $\boldsymbol{C}_A$	$\sigma_{\tilde{G}_{\text{LS}}}$	6.6	dB
	$\sigma_{\tilde{K}}$	3	dB
	$\sigma_{\tilde{\sigma}_\tau}$	1.6	dB
	$\rho_{\tilde{G}_{\text{LS}}\tilde{K}}$	0.74	—
	$\rho_{\tilde{G}_{\text{LS}}\tilde{\sigma}_\tau}$	−0.39	—
	$\rho_{\tilde{K}\tilde{\sigma}_\tau}$	−0.45	—
standard deviations and corr. coeff. for $\boldsymbol{C}_B$	$\sigma_{\tilde{G}_{\text{LS}}}$	3.1	dB
	$\sigma_{\tilde{K}}$	3.2	dB
	$\sigma_{\tilde{\sigma}_\tau}$	1.4	dB
	$\rho_{\tilde{G}_{\text{LS}}\tilde{K}}$	0.5	—
	$\rho_{\tilde{G}_{\text{LS}}\tilde{\sigma}_\tau}$	−0.22	—
	$\rho_{\tilde{K}\tilde{\sigma}_\tau}$	−0.18	—
correlation distances	$(\Delta d)_{\text{c, LS}}$	20.2	m
	$(\Delta d)_{\text{c, }K}$	5.5	m
	$(\Delta d)_{\text{c, }\sigma_\tau}$	14.6	m

[a] Decibels relative to 1 s.

the existing models in three different types, tap-delay models, ray-based models and geometry-based stochastic models. The authors highlight that tap-delay models do not directly take into consideration the time variations of the channel typical for vehicular scenarios. Furthermore, ray-based models often lead to time-consuming simulations, when many rays are taken into account. The authors claim that a statistical approach is often needed to yield a representative behaviour of the dynamics in VANETs and that it has the potential to yield reasonable simulation times. This is one reason for why a geometry-based stochastic channel model is often to prefer in network analysis. In [7], a summary of existing channel modelling and measurements especially for vehicle-to-vehicle (V2 V) applications is also presented.

In [8], the authors discuss the need of a more detailed description of the physical layer to be used for network simulations. The purpose is to improve the quality of the results from network simulations and they claim that the basic threshold reception model in order to simulate the carrier sense functionality and determine successful reception is not adequate. It is especially interference because of collisions that is difficult to take into consideration without a more detailed description of the physical layer. Furthermore, the NS-2 simulator that the authors refer to as not having a proper threshold reception model is using relatively simple channel models, that is, the simulator uses either a free-space model, a two-ray ground reflection model or a shadowing model. On the basis of these reasons the authors suggest network simulations on bit level. To improve the quality of the network results with reasonable computational complexity, another approach is to develop a channel model with appropriate behaviour that provides accurate estimates of the signal-to-noise ratio (SNR) to be used in the network simulations.

In this paper, we propose a model structure that is able to capture the essence of the channel characteristics and that copes with the constraint of low computational complexity when used in network simulations. For network performance analysis, the particular geographical location is generally not interesting, as long as the statistical description meets the considered environment to be used in. The proposed model is a scenario-based stochastic channel model and it is similar to a geometry-based stochastic channel model in the sense that the channel statistics varies over positions. The model includes different environment-dependent channel parameters that control the distributions as the large-scale fading, the Rician K-factor and the delay spread. In this paper, model parameters are exemplified for an urban peer-to-peer scenario at 300 MHz. However, the model framework can be used for other environments and other frequency bands as long as the statistics for the channel parameters are available. Also results from a deterministic channel model are possible to use for derivation of the needed channel parameters. The proposed model has similarities with other existing models, as, for example, the one proposed in [9]. However, our model also considers the correlation between the channel parameters, and a first-order autoregressive (AR) filter is used to maintain accurate spatial correlation during terminal movement. We also demonstrate the behaviour of the proposed stochastic channel model in terms of the statistical behaviour of the channel parameters and by showing two typical examples of results at link and network levels.

The remainder of this paper is organised as follows. Section 2 describes the proposed channel model structure, including the distance-dependent path gain, large-scale and small-scale fading. It also describes the incorporation of correlation between large-scale parameters and the spatial correlation. Section 3 describes an example of parameter generation based on channel measurements. Section 4 exemplifies the impact of using the proposed channel model, both on link level and on network level. Comparisons are performed with measurement data and a plain two-ray ground model. Furthermore, the statistical characteristics of the channel parameters are examined. Finally, Section 5 concludes this paper.

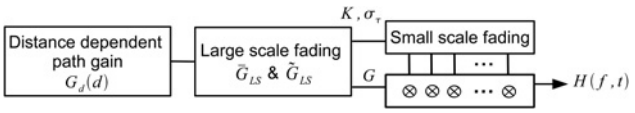

Fig. 1 *Stochastic channel model structure*

2 Channel model

To evaluate multiple access control (MAC) solutions and routing protocols for MANETs by use of simulations, the dynamics of the radio channels must be properly modelled. Current channel models for network evaluations are in their most simple form based on the distance between transmitter and receiver (e.g. a plain-earth model) to more thorough models with ray-tracing wave propagation simulations for each link. The former ones do not consider environmental effects such as fading properties, whereas the later models, in their most sophisticated form, can become very computationally demanding. In [10, 11], the small- and large-scale fading have been shown to significantly affect the performance of *ad hoc* networks. Furthermore, the correlation in time, space and frequency is often important when studying network performance. For example, when analysing the link availability in time for network protocols with fast acknowledgements, the behaviour of the channel dynamics is of great importance.

2.1 Proposed channel model structure

To address a dynamic channel behaviour (the large- and small-scale fading and the correlation properties), we propose the channel model structure shown in Fig. 1; the parameters are explained later in this section. The model is divided in three different blocks, where each block determines one layer of the total channel fading process.

- The first block includes the distance-dependent path gain $G_{\mathrm{d}}(d)$, where d is the geometrical distance between two MANET nodes. Here, $G_{\mathrm{d}}(d)$ is computed from an empirically developed link attenuation model.
- The second block creates the large-scale channel variations. This includes the large-scale (slow) fading G_{LS}, which are the path gain variations relative to $G_{\mathrm{d}}(d)$. In addition, other large-scale parameters are generated to control the small-scale fading process in the third block. Examples of such parameters are the root-mean-square (RMS) delay spread σ_τ and the Rician K-factor, which are related to the coherence bandwidth and the amplitude distribution of the small-scale fading, respectively.
- The third block considers the small-scale fading process with a Rician amplitude distribution. The small-scale variations are created for multiple subchannels, whose mutual correlation depends on the coherence bandwidth. Finally, the small-scale fading process is multiplied with the large-scale fading obtained in block two to conduct the total fading.

These three blocks constitutes the base of the model. The radio channel in position $\boldsymbol{r}$ can be characterised by the frequency selective transfer function as

$$H(f, \boldsymbol{r}) = \sqrt{G(\boldsymbol{r})}Y(f, \boldsymbol{r}) \tag{1}$$

where $G(\boldsymbol{r})$ (expressed in linear scale in (1)) is the link's composite path gain, which can be obtained from

$$G(\boldsymbol{r}) = G_{\mathrm{d}}(d) + G_{\mathrm{LS}} \quad [\mathrm{dB}] \tag{2}$$

and where f and $Y(f, \boldsymbol{r})$ are the frequency of interest and the complex-valued small-scale fading in position $\boldsymbol{r}$, respectively; the latter is described in Section 2.4. Furthermore, in (2), $G_{\mathrm{d}}(d)$ is

doi: 10.1049/joe.2014.0277

the distance-dependent path gain, see Section 2.2, and G_{LS} is the large-scale fading, see Section 2.3.

A similar approach to model the channel fading, with a similar block structure, has been proposed in [9] for wireless personal area networks for indoor use. However, we impose the small-scale fading in the frequency-transfer function instead of adding a time-domain component. Moreover, the incorporation of the correlation between large-scale channel parameters differs from what is proposed in [9].

2.2 Distance-dependent path gain

The distance-dependent path gain $G_{\mathrm{d}}(d)$, generated in the first block shown in Fig. 1, is modelled to be a function of the geometrical distance d as

$$G_{\mathrm{d}}(d) = G_0 - 10n\log_{10}\left(\frac{d}{d_{\mathrm{ref}}}\right)\,[\mathrm{dB}] \tag{3}$$

where G_0 is the path gain at the reference distance d_{ref} and n is the path-gain exponent.

2.3 Large-scale fading

For the large-scale channel variation, three important parameters are modelled. The parameter G_{LS} is the large-scale fading, K and σ_τ are the K-factor and the channels RMS delay spread, respectively. The large-scale parameters are defined as

$$\begin{pmatrix} G_{\mathrm{LS}} \\ K \\ \sigma_\tau \end{pmatrix} = \begin{pmatrix} \overline{G}_{\mathrm{LS}} \\ \overline{K} \\ \overline{\sigma}_\tau \end{pmatrix} + \begin{pmatrix} \widetilde{G}_{\mathrm{LS}} \\ \widetilde{K} \\ \widetilde{\sigma}_\tau \end{pmatrix} + \begin{pmatrix} \mu_{G_{\mathrm{LS}}} \\ \mu_K \\ \mu_{\sigma_\tau} \end{pmatrix} \tag{4}$$

All parameters in (4) are expressed in logarithmic units. The two components $\overline{(\cdot)}$ and $\widetilde{(\cdot)}$ are the local mean and the superimposed variation around the local mean, respectively. The last term $\boldsymbol{\mu} = [\,\mu_{G_{\mathrm{LS}}} \quad \mu_K \quad \mu_{\sigma_\tau}\,]^{\mathrm{T}}$ is the global mean for each channel parameter and is valid for a whole scenario and can be seen as an offset factor. The local mean $\overline{(\cdot)}$ on the contrary varies at a quite large spatial scale and can typically be considered constant over one block in an urban scenario. The superimposed variation $\widetilde{(\cdot)}$ depends mainly on the local environment in the vicinity of the radio nodes; its spatial scale is therefore considerably smaller.

The proposed structure in (4) is based on the findings in [12], where it was stated that $\overline{(\cdot)}$ and $\widetilde{(\cdot)}$ can be considered as approximately normal distributed. By dividing each parameter's variation into the two separate components $\overline{(\cdot)}$ and $\widetilde{(\cdot)}$, we can handle the different spatial scales of the variation more easily. Furthermore, the analysis of the results from the urban measurements in [12] showed that there is a dependency between the channel parameters. To consider the correlation between the large-scale parameters, covariance matrices are introduced. If we let $\bar{\boldsymbol{\Omega}} = [\,\bar{G}_{\mathrm{LS}} \;\; \bar{K} \;\; \bar{\sigma}_\tau\,]^{\mathrm{T}}$ and $\tilde{\boldsymbol{\Omega}} = [\,\tilde{G}_{\mathrm{LS}} \;\; \tilde{K} \;\; \tilde{\sigma}_\tau\,]^{\mathrm{T}}$, where $(\cdot)^{\mathrm{T}}$ denotes the transpose operator, we can generate correlated realisations of these parameters as

$$\bar{\boldsymbol{\Omega}} = \boldsymbol{C}_A^{1/2}\boldsymbol{x} \tag{5}$$

$$\tilde{\boldsymbol{\Omega}} = \boldsymbol{C}_B^{1/2}\boldsymbol{y} \tag{6}$$

where $\boldsymbol{C}_A$ and $\boldsymbol{C}_B$ are the covariance matrices for parameter vectors $\bar{\boldsymbol{\Omega}}$ and $\tilde{\boldsymbol{\Omega}}$, respectively, and the matrix square root is defined so that $\boldsymbol{C} = \boldsymbol{C}^{1/2}\boldsymbol{C}^{1/2}$. The elements of $\boldsymbol{x}$ and $\boldsymbol{y}$ are independent normal-distributed variables with zero mean and unit variance. As $\boldsymbol{x}$ and $\boldsymbol{y}$ are modelled as zero-mean processes, the global mean $\boldsymbol{\mu}$ must be added in (4) to obtain the correct level of the large-scale parameters.

On the basis of measurement analysis, Gudmundson [13] proposed the autocorrelation properties of the large-scale fading process to be modelled by a simple exponential function. This is attractive from a computational point of view because the fading process can be generated by filtering a white Gaussian noise process through an AR filter. In our proposed model, we assume that the autocorrelation functions for all large-scale parameters can be modelled by an exponential function. Hence, for a generic element $\tilde{\Omega}$ of the mutually correlated parameters in vector $\tilde{\boldsymbol{\Omega}}$ in (6), a sequence of spatially correlated realisations of that channel parameter $\tilde{\Omega}_F(\boldsymbol{r}_p)$, $p = 1, \ldots, P$, is generated as

$$\tilde{\Omega}_F(\boldsymbol{r}_p) = \begin{cases} \alpha_p\,\tilde{\Omega}_F(\boldsymbol{r}_{p-1}) + \sqrt{1-\alpha_p^2}\,\tilde{\Omega}_p\,, & \text{if } 2 \le p \le P \\ \tilde{\Omega}_p\,, & \text{if } p = 1 \end{cases} \tag{7}$$

where $\boldsymbol{r}_p$ is the pth position, $\tilde{\Omega}_p$ is a realisation from (6) and α_p is a coefficient that determines the statistical dependency between $\tilde{\Omega}_F(\boldsymbol{r}_p)$ and $\tilde{\Omega}_F(\boldsymbol{r}_{p-1})$. Under the assumption of local wide-sense stationarity, α_p can be expressed as

$$\alpha_p = \rho_p(\Delta d) \tag{8}$$

where $\Delta d = |\boldsymbol{r}_p - \boldsymbol{r}_{p-1}|$ is the distance between two adjacent positions and ρ_p is an autocorrelation function that is valid within a local area around $\boldsymbol{r}_p$. On the basis of the assumption of an exponential autocorrelation, we let

$$\rho_p(\Delta d) = \left(\frac{1}{c}\right)^{-\Delta d/(\Delta d)_{\mathrm{c}}} \tag{9}$$

where $(\Delta d)_{\mathrm{c}}$ is the correlation distance at correlation level c. In (9), the correlation distance is implicitly dependent on $\boldsymbol{r}_p$.

To summarise the methodology, the large-scale parameters can be generated as follows:

(1) Generate the covariance matrices $\boldsymbol{C}_A$ and $\boldsymbol{C}_B$ based on parameters from a reference scenario.
(2) Generate the local mean values $\bar{\boldsymbol{\Omega}}$ for G_{LS}, K and σ_τ according to (5).
(3) Generate the superimposed process $\tilde{\boldsymbol{\Omega}}$, (6), and filter it according to (7) to incorporate the spatial correlation.
(4) Determine the scenario dependent global mean value $\boldsymbol{\mu}$.
(5) Compute the combined large-scale result according to (4).

From (4), the G_{LS} is used in (2), whereas K and σ_τ are used in the derivation of the small-scale fading.

2.4 Small-scale fading

In general, the small-scale fading process $Y(f, \boldsymbol{r})$ is characterised by its distribution and by its frequency and spatial correlation properties. In our model, we assume that $Y(f, \boldsymbol{r})$ is Rician distributed and that the time dispersion of the channel can be described as a superposition of a dense multipath component (with an exponentially decaying delay power spectrum), and a specular component. To simplify the model, we make the approximation that the realisations are spatially independent if $|\boldsymbol{r}_p - \boldsymbol{r}_{p-1}| \ge d_\varepsilon$ (a certain threshold distance); if the movement is $< d_\varepsilon$, we assume that $Y(f, \boldsymbol{r}_p) = Y(f, \boldsymbol{r}_{p-1})$. In this way, the effects of static nodes are captured.

Following the modelling approach for dense multipath components in [14–16], we let the dense multipath components have the

delay power spectrum

$$S_{\mathrm{dm}}(\tau)=\begin{cases}0, & \text{if } \tau<\tau_0\\ \dfrac{a_1}{b_1}\exp\left(-\dfrac{\tau-\tau_0}{b_1}\right), & \text{if } \tau\geq\tau_0\end{cases} \tag{10}$$

where τ_0 is the delay of the first arriving multipath component, b_1 is the decay constant of the power spectrum and a_1 is the total dense multipath power; for the brevity of notation, we have dropped the explicit dependency on $\boldsymbol{r}$ in the equation. The specular component (which is assumed to be statistically independent of the dense multipath components) has the delay power spectrum

$$S_{\mathrm{sc}}(\tau)=a_0\,\delta(\tau-\tau_0) \tag{11}$$

where a_0 is the power of the specular component, and again the dependency on $\boldsymbol{r}$ is dropped for brevity.

The frequency autocorrelation function for the dense multipath components $\psi_{\mathrm{dm}}(\Delta f)$ is obtained by a Fourier transformation of (10) as

$$\psi_{\mathrm{dm}}(\Delta f)=\frac{a_1}{1+\mathrm{j}2\pi\Delta f b_1}\exp(-\mathrm{j}2\pi\Delta f\tau_0) \tag{12}$$

where a_1 and b_1 are determined by the Rician K-factor and the delay spread. Under the power constrain $a_0+a_1=1$, the parameters a_0, a_1 and b_1 in (10)–(12) can be expressed, respectively, as

$$a_0=\frac{K}{K+1} \tag{13a}$$

$$a_1=\frac{1}{K+1} \tag{13b}$$

$$b_1=\frac{\sigma_\tau}{\sqrt{1-a_0^2}} \tag{13c}$$

Finally, with the explicit dependency on $\boldsymbol{r}$ reintroduced, we can now write the small-scale fading process $\boldsymbol{y}(\boldsymbol{r}_p)=[Y(f_1,\,\boldsymbol{r}_p)Y(f_2,\,\boldsymbol{r}_p),\,\ldots,\,Y(f_{n_f},\,\boldsymbol{r}_p)]^{\mathrm{T}}$ at discrete frequency points $f_1, f_2, \ldots, f_{n_f}$ as

$$\boldsymbol{y}(\boldsymbol{r}_p)=\sqrt{\frac{K(\boldsymbol{r}_p)}{K(\boldsymbol{r}_p)+1}}+\sqrt{\frac{1}{K(\boldsymbol{r}_p)+1}}\boldsymbol{C}_f^{1/2}(\boldsymbol{r}_p)\boldsymbol{w}_p \tag{14}$$

where the elements of $\boldsymbol{w}_p$ are independent identically distributed complex Gaussian stochastic variables with zero mean and unit variance, and $\mathbf{C}_{\mathrm{f}}(\boldsymbol{r}_p)$ is the frequency correlation matrix with elements

$$\left[\boldsymbol{C}_{\mathrm{f}}\right]_{kl}=\frac{1}{a_1}\psi_{\mathrm{dm}}(f_k-f_l) \tag{15}$$

The two large-scale parameters $K(\boldsymbol{r}_p)$ and $\sigma_\tau\,(\boldsymbol{r}_p)$ that govern the statistics of the small-scale fading are obtained from (7), and $\tau_0(\boldsymbol{r}_p)$ is computed from the geometrical path length of the link.

2.5 *Model simplifications*

Modern wideband radio systems usually apply advance modulation and coding schemes. Such systems can take advantage of multipath propagation, and obtain diversity gains on frequency selective radio channels. Therefore, the performance of such systems mainly depends on the instantaneous SNR, averaged over the operating bandwidth. Under such assumptions, it is possible to reduce the computational complexity of the proposed model even further by simplifications to be used in small-scale fading calculations and hence reduce the complexity and simulation time, as well.

The diversity order that can be extracted by an idealised receiver system can be approximated as $m=W_{\mathrm{s}}/W_{\mathrm{coh}}$, where W_{s} and W_{coh} are the system bandwidth and the coherence bandwidth of the channel, respectively.

Hence, m can be viewed as the number of independently fading subchannels, which makes the frequency correlation matrix $\boldsymbol{C}_{\mathrm{f}}$ in (14) to become an identity matrix $\boldsymbol{I}_m$. Then, the instantaneous SNR is obtained from the wideband path-gain $G_{\mathrm{wb}}(\boldsymbol{r})$, which is computed as

$$G_{\mathrm{wb}}(\boldsymbol{r}_p)=G(\boldsymbol{r}_p)+10\log_{10}\|\,\boldsymbol{y}(\boldsymbol{r}_p)\,\|^2\ \ [\mathrm{dB}] \tag{16}$$

where $\|\cdot\|$ denotes the Euclidean norm and $G(\boldsymbol{r}_p)$ is the composite path gain, according to (2).

3 Example of parameterisation of the model by using an urban scenario

Parameters for the proposed model have in this paper been extracted from a peer-to-peer measurement campaign at 300 MHz in an urban environment; for further details and results, see [12]. However, the model framework can be used for other environments and other frequency bands as long as such channel measurements for such conditions are available. The measurement campaign was conducted in the city centre of the fifth largest city in Sweden, which with international standards is a rather small town. Fig. 2 shows an aerial photo of the measurement area. This part of the town, which typically has three- to six-storey buildings, is rather flat but slopes gently towards the river on the east side. The transmitter Tx and the receiver Rx were both placed on vehicles with the antenna arrays mounted on top of each vehicle. The antenna heights were ∼1.8 and 2.1 m above the ground for the Tx and Rx, respectively. The scenario consists of 3 different Tx locations (Tx1, Tx2, Tx3) and from each Tx location, 25 Rx routes (Rx1–Rx25) were conducted. During the measurements the Tx was stationary at each site, whereas the Rx was driven along the measurement routes. The measurements were performed at a centre frequency of 285 MHz with a 20 MHz wide probing signal.

On the basis of the large set of measured channel transfer functions derived from the measurement campaign, the parameters of the proposed model can be generated in accordance with Section 2, see Table 1.

We can, for example, see that the distance-dependent path-gain exponent n for this scenario is 4.15. Furthermore, in the same table, we show the extracted parameters for the standard deviations and cross-correlation coefficients of our two three-dimensional large-scale processes $\bar{\boldsymbol{\Omega}}$ and $\tilde{\boldsymbol{\Omega}}$; that is, the local mean and the superimposed process, respectively. From the parameters in the table, we can compute the covariance matrices $\boldsymbol{C}_A$ and $\boldsymbol{C}_B$, used in (5) and (6), respectively, according to

$$\boldsymbol{C}_A=\begin{bmatrix}\sigma^2_{\bar{G}_{\mathrm{LS}}} & \rho_{\bar{G}_{\mathrm{LS}}\bar{K}}\sigma_{\bar{G}_{\mathrm{LS}}}\sigma_{\bar{K}} & \rho_{\bar{G}_{\mathrm{LS}}\bar{\sigma}_\tau}\sigma_{\bar{G}_{\mathrm{LS}}}\sigma_{\bar{\sigma}_\tau}\\ \rho_{\bar{G}_{\mathrm{LS}}\bar{K}}\sigma_{\bar{G}_{\mathrm{LS}}}\sigma_{\bar{K}} & \sigma^2_{\bar{K}} & \rho_{\bar{K}\bar{\sigma}_\tau}\sigma_{\bar{K}}\sigma_{\bar{\sigma}_\tau}\\ \rho_{\bar{G}_{\mathrm{LS}}\bar{\sigma}_\tau}\sigma_{\bar{G}_{\mathrm{LS}}}\sigma_{\bar{\sigma}_\tau} & \rho_{\bar{K}\bar{\sigma}_\tau}\sigma_{\bar{K}}\sigma_{\bar{\sigma}_\tau} & \sigma^2_{\bar{\sigma}_\tau}\end{bmatrix} \tag{17}$$

and

$$\boldsymbol{C}_B=\begin{bmatrix}\sigma^2_{\tilde{G}_{\mathrm{LS}}} & \rho_{\tilde{G}_{\mathrm{LS}}\tilde{K}}\sigma_{\tilde{G}_{\mathrm{LS}}}\sigma_{\tilde{K}} & \rho_{\tilde{G}_{\mathrm{LS}}\tilde{\sigma}_\tau}\sigma_{\tilde{G}_{\mathrm{LS}}}\sigma_{\tilde{\sigma}_\tau}\\ \rho_{\tilde{G}_{\mathrm{LS}}\tilde{K}}\sigma_{\tilde{G}_{\mathrm{LS}}}\sigma_{\tilde{K}} & \sigma^2_{\tilde{K}} & \rho_{\tilde{K}\tilde{\sigma}_\tau}\sigma_{\tilde{K}}\sigma_{\tilde{\sigma}_\tau}\\ \rho_{\tilde{G}_{\mathrm{LS}}\tilde{\sigma}_\tau}\sigma_{\tilde{G}_{\mathrm{LS}}}\sigma_{\tilde{\sigma}_\tau} & \rho_{\tilde{K}\tilde{\sigma}_\tau}\sigma_{\tilde{K}}\sigma_{\tilde{\sigma}_\tau} & \sigma^2_{\tilde{\sigma}_\tau}\end{bmatrix} \tag{18}$$

where σ_X^2 is the variance of X and ρ_{XY} is the cross-correlation

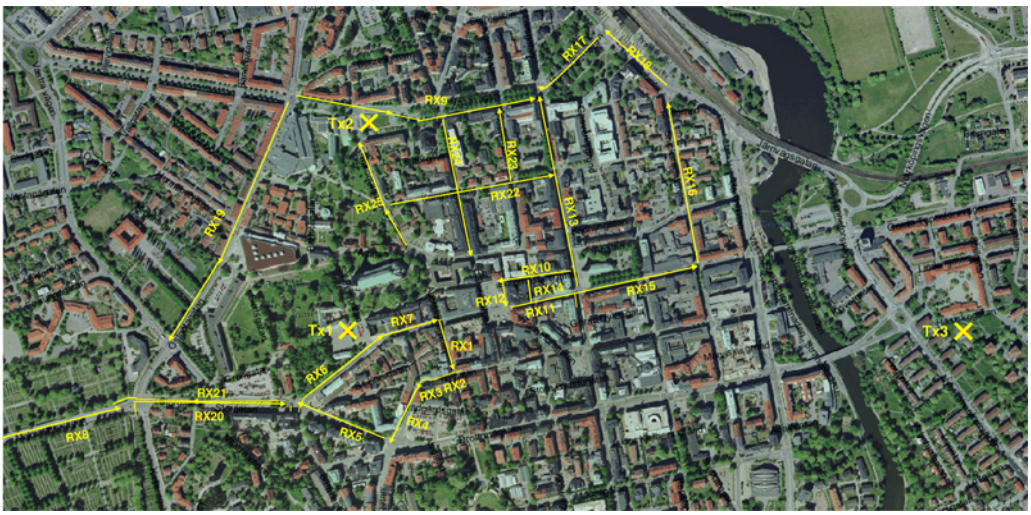

Fig. 2 *Measurement area in the city centre of Linkoping, Sweden. Transmitter sites (crosses) and receiver routes*

coefficient defined as

$$\rho_{XY} = \frac{\mathrm{cov}(X,\ Y)}{\sigma_X \sigma_Y} = \frac{E((X-\mu_X))(Y-\mu_Y))}{\sigma_X \sigma_Y} \tag{19}$$

in which $\mathrm{cov}(X,\ Y)$ denotes the covariance between X and Y.

From the urban measurements, the mean value of the correlation distance $(\Delta d)_c$ in (9) has been calculated for respective large-scale channel parameter at a correlation level $c = 0.5$. The correlation distances are also given in Table 1.

4 Example of the channel model behaviour

In the following, we will exemplify the behaviour of the proposed stochastic channel model. Firstly, we compare the distributions of model-generated large-scale parameters with the parameters derived from measurements directly. Secondly, we study the performance on link level in an *ad hoc* network in terms of probability that the SNR exceeds a certain threshold, which corresponds to the SNR requirement of a certain service. The performance results obtained for the proposed stochastic channel model are compared with the results for a simple two-ray model as well as results based on channel measurements. Finally, we will study the network performance of a simulated *ad hoc* network in an urban environment. The proposed stochastic channel model is used to generate the maximum data rate possible for the instantaneous channel conditions of the links. Hence, different kinds of routing algorithms can be evaluated. With this approach, the network performance in terms of the probability of packet delivery ratio is analysed for networks of different connectivities.

4.1 Statistical properties of the channel parameters

To verify the statistics of the modelled large-scale channel variations, we compare the cumulative distribution functions (CDFs) of the generated channel parameters in (4) – that is, large-scale fading G_{LS}, Rician K-factor and RMS delay spread σ_τ – with the CDFs that were computed from the measured data. In Figs. 3–5, the CDFs of the large-scale channel parameters are shown for measurements and for the proposed channel model. The curves denoted 'Measurements' are derived from the measurements directly, considering all combinations of transmitter and receiver positions, see [12]. The corresponding curves denoted 'Model' are derived from simulations with the proposed channel model, for the same

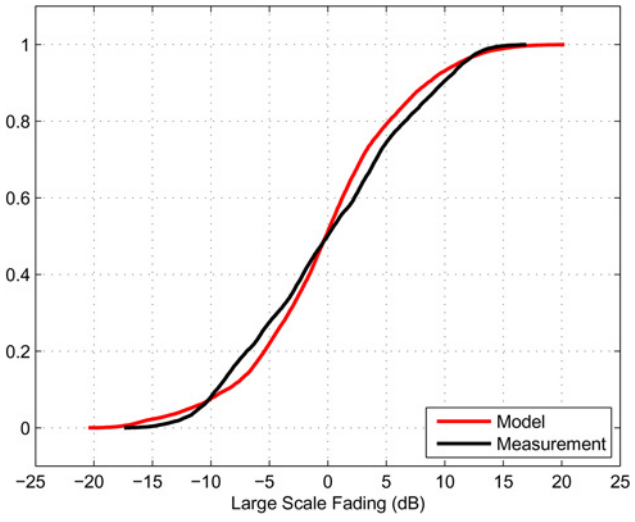

Fig. 3 *CDFs for the large-scale fading G_{LS} in dB*

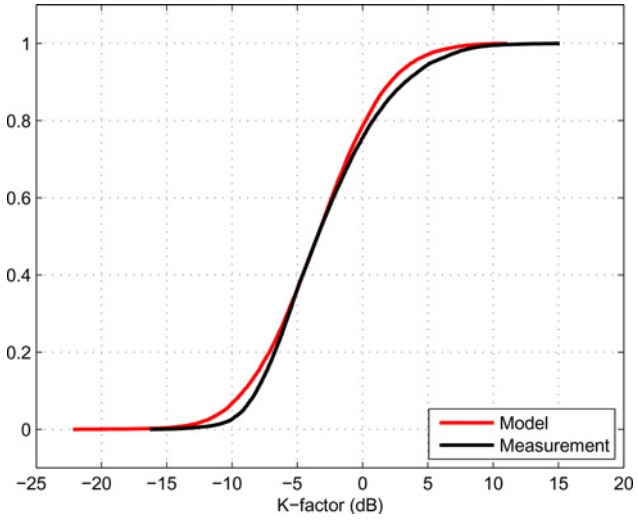

Fig. 4 *CDFs for the K-factor in dB*

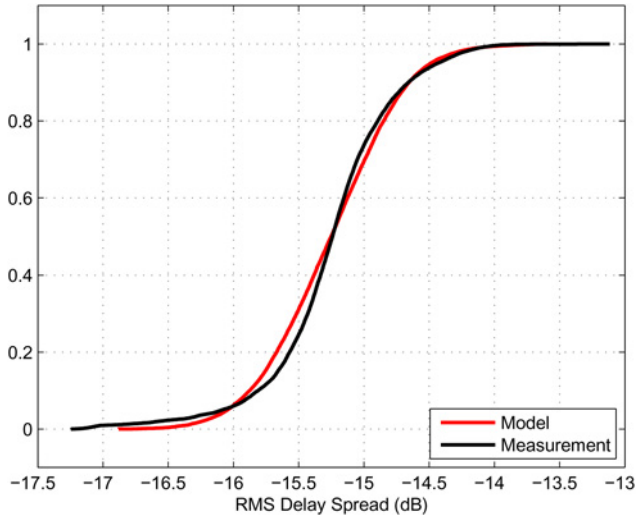

Fig. 5 *CDFs for the RMS delay spread σ_τ. (Expressed as $\log_e(\sigma_\tau)$)*

distributions of the distances. In these figures, we can see that the agreement between the CDFs for the parameters generated by the model and the CDFs from the measured data is quite good for all three parameters. This justifies the proposed distributions in the second block of the model structure, see Fig. 1.

4.2 *Channel model behaviour on link level in an* ad hoc *network*

To study the link performance in a MANET, channel realisations are obtained from the proposed channel model, and compared with the performance obtained when directly measured channels are used. For this purpose, a network is created from a subset of the measurement routes [17], with the consequence that the mobility is determined from the available measurement positions. To be specific, the node positions are the same as the Tx and Rx positions in the measurements.

We use a link model that have two different states, that is, if the SNR is larger than a certain SNR threshold, the link is considered to function, otherwise to fail. Generally, the SNR threshold depends on the specific radio communication system and service requirement. This is a reasonable approximation when considering a system that utilises strong channel coding. Such a system will have a sharp threshold behaviour, where the message error probability goes from one to a negligible level within a narrow SNR range. The use of this link model is a common approach to determine link performance in network simulations [1] and is usually needed to limit the computational time. The proposed stochastic channel model is used to derive the probability that the SNR will exceed the threshold for the same node movements as for the created network based on the measured links. The probability that the SNR exceeds the threshold is shown in Fig. 6 for the created network with the measured links and with the proposed channel model. In addition, the result for a simple two-ray model [18] is included in this figure, for comparison. The two-ray model is an example of a simple channel model, which is commonly used in many network simulation tools. We can see that the results with the simple two-ray model exhibit a typical threshold behaviour with transition at a certain distance. This distance corresponds to the SNR threshold, where the transition from acceptable link performance to a not acceptable link performance appears. In contrast to the results of the two-ray model, the probability that the SNR will exceed the threshold for the measurements and the proposed channel does not exhibit a distinct transition and assumes values between zero and one for a large range of distances. Furthermore, we can see that the overall behaviour of the probability that the SNR will exceed the threshold derived from the proposed channel model and the measurements have a similar variability. However, the results with the stochastic channel model and the measurements differ, since the results for the measurements are based on a subset of the measurement campaign, whereas the results for the stochastic channel model are based on the whole measurement campaign results.

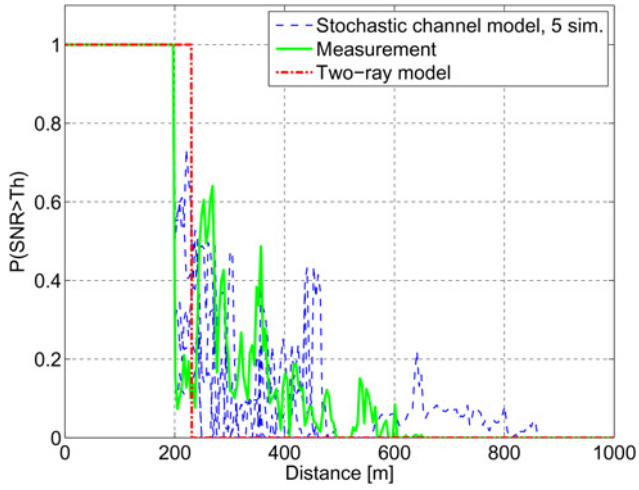

Fig. 6 *Probability that SNR exceeds a certain threshold as a function of distance*

4.3 *Channel model behaviour on network level*

To exemplify how the choice of channel model, and its degree of details, can affect the network performance, we have simulated a mobile scenario with 64 nodes. In that scenario, we assume that the nodes are moving around for 400 s in an 8×8 km square area at a speed of 50 km/h. To model the movements of the nodes, we use the random walk model in [17]. According to the mobility model, all nodes move independently of each other and, if a node hits the boundary of the square, it bounces back like a ball. The user traffic is modelled as broadcast transmissions of packets. A source is randomly selected among the 64 nodes to send one packet. Thereafter, a new source is randomly selected and so on. A basic time-division multiple access MAC protocol is used for the simulations. Therefore no robustness issues have to be addressed at the MAC layer because of packet collisions. For such protocols, the time is divided into time slots that are grouped into repeating frames. Each node is assigned one time slot in each frame and the traffic in the network is kept sufficiently low to avoid congestion in the network. To route the packets in the network, we use the multi-point-relay (MPR) method according to the simplified multicast forwarding framework [19], and the MPR selection mechanisms are the optimised link state routing protocol [20]. Both user and overhead traffic are transmitted in the network.

For the network simulations, we use an in-house developed radio network simulator. On the basis of the channel realisation, when a packet is sent, the SNR and the instantaneous channel capacity is computed and used to decide whether a packet can be correctly received in a node or not. If the experienced channel capacity is higher than the data rate, the packet is assumed to be correctly received. Note, that in reality no system will reach the channel capacity; there will always be some implementation losses. However, such losses are neglected in these simulations as our focus is merely on the channel behaviour and its influence on the network performance.

The performance is studied in terms of delivery ratio, defined as the fraction of packets that reach the destinations. A packet that is not reaching the destination is lost either because no route exists or that a link deteriorates so that a transmitted packet cannot be

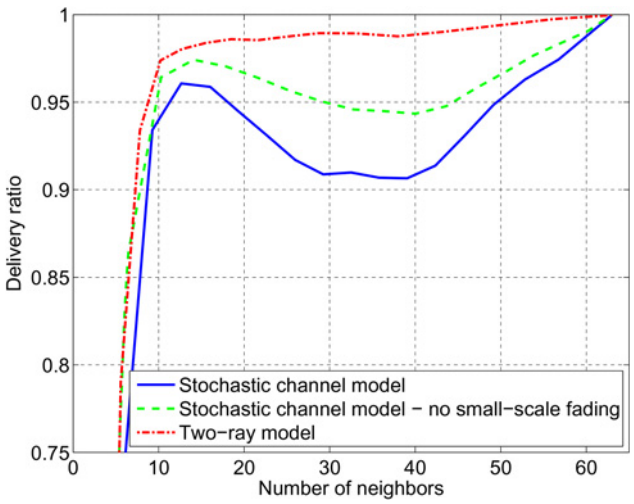

Fig. 7 *Delivery ratio as a function of the network connectivity*

received. No acknowledgments or automatic repeat request mechanisms are used on the link level, that is, between a specific transmitter and receiver. The delivery ratio should be high (say, over 95%) to assure a satisfactory quality of service. The delivery ratio is calculated for different network connectivities. As a measure of the network connectivity, we use the number of one-hop-neighbours any given node has in average measured at MAC layer. The average value is taken over all the transmissions from all the nodes during one simulation run. To obtain different network connectivities, we adjust the output power of the nodes in the scenario and hence different network situations are created from a sparse to a dense network.

To illustrate how the choice of channel model, and how its degree of details can affect the result, we compare the network performance when using different channel models. In Fig. 7, the delivery ratio is shown as a function of the network connectivity, measured as the average number of one-hop-neighbours. The proposed channel model and the two-ray model are used for the network simulations. To further investigate the effects of the channel dynamics, the proposed model without small-scale fading is included as an intermediate detailed model. Unfortunately, measurements of the actual links are generally not possible in reality to use in the network simulations with random movement and a large number of the nodes, as was possible in the link level example in previous section. For example, our scenario with 64 nodes would imply 2016 instantaneous links that are moving randomly and need to be updated with a high rate. There are some of the reasons of why a stochastic channel model is urgent for network simulations.

This figure shows results for the different channel models, the two-ray model, the proposed channel model without small-scale fading and the proposed channel model with small-scale fading, which are models with an increasing degree of detailed channel description. In the simulations, the delivery ratio is between 90 and 100% for networks with over ten node neighbours. This is in the critical region of acceptable performance (a critical value of delivery ratio is often near 95%). Hence, it is particularly important with proper modelling of the channel to obtain accurate estimates of the delivery ratio. From the simulations, we can see that the values of the delivery ratio, for the three channel descriptions, do not differ substantially. Furthermore, when the level of model details increases, the delivery ratio decreases. The simple two-ray model deceptively yields a higher delivery ratio than what the proposed channel model gives. Additionally as can be seen, the largest differences in the results between the proposed channel model and the two-ray ground model occur when the nodes have 30–40 neighbours. This difference is a consequence of the inherent robustness of the used broadcasting method, that is, the number of redundant MPRs is reduced when the number of neighbours increases. For these network types, the probability decreases of having an alternative route when a link disappears. This leads to a larger impact from the fading on the delivery ratio. The overall conclusion is that the network simulation results benefit from a more detailed channel description than the two-ray model can offer. Furthermore, the small-scale fading needs to be incorporated in the model when analysing the network performance.

5 Conclusions

There is a need for more realistic channel models for analysis of *ad hoc* network performance. The channel model must include both large-scale and small-scale fading as an effect from the mobility of the network terminals. In this paper, a model structure is proposed that captures the essence of the channel characteristics and copes with the constraint of low computational complexity. The fading statistics of the model are determined by a number of parameters that describe the distributions of the large-scale fading, the Rician K-factor and the delay spread. The model considers the mutual correlation between the channel parameters and the spatial correlation of the parameters. Examples justify that the proposed channel model, with model parameters estimated from urban peer-to-peer scenario at 300 MHz, models the channel dynamics appropriately when analysing the link and network performance.

6 References

[1] Stanica R., Chaput E., Beylot A.-L.: 'Simulation of vehicular ad-hoc networks: challenges, review of tools and recommendations', *Comput. Netw.*, 2011, **55**, (14), pp. 3179–3188

[2] Zang L.F., Rowe G.B.: 'Improved modelling for ad-hoc networks', *Electron. Lett.*, 2007, **43**, (21), pp. 1156–1157

[3] Zhao M., Wang W.: 'The impacts of radio channel and node mobility on link statistics in mobile ad hoc networks'. Proc. IEEE Globecom 2007, Washington, USA, November 2007

[4] Chapin J., Chan V.: 'The next 10 years of DOD wireless networking research'. 2011–Milcom 2011 Military Communications Conf., November 2011, pp. 2238–2245

[5] Wang L.-C., Liu W.-C., Cheng Y.-H.: 'Statistical analysis of a mobile-to-mobile Rician fading channel model', *IEEE Trans. Veh. Technol.*, 2009, **58**, (1), pp. 32–38

[6] Mecklenbrauker C., Molisch A., Karedal J., *ET AL.*: 'Vehicular channel characterization and its implications for wireless system design and performance', *Proc. IEEE*, 2011, **99**, (7), pp. 1189–1212

[7] Wang C.-X., Cheng X., Laurenson D.: 'Vehicle-to-vehicle channel modeling and measurements: recent advances and future challenges', *IEEE Commun. Mag.*, 2009, **47**, (11), pp. 96–103

[8] Mittag J., Papanastasiou S., Hartenstein H., Strom E.: 'Enabling accurate cross-layer PHY/MAC/NET simulation studies of vehicular communication networks', *Proc. IEEE*, 2011, **99**, (7), pp. 1311–1326

[9] Karedal J., Johansson A.J., Tufvesson F., Molisch A.F.: 'A measurement-based fading model for wireless personal area networks', *IEEE Trans. Wirel. Commun.*, 2008, **7**, (11), pp. 4575–4585

[10] Gray R.S., Kotz D., Newport C., *ET AL.*: 'Outdoor experimental comparison of four ad hoc routing algorithms'. Proc. of the ACM/IEEE Int. Symp. on Modeling, Analysis and Simulation of Wireless and Mobile Systems (MSWiM), 2004, pp. 220–229

[11] Kiess W., Mauve M.: 'A survey on real-world implementations of mobile ad-hoc networks', *Ad Hoc Netw.*, 2007, **5**, (3), pp. 324–339 [Online]. Available at http://www.sciencedirect.com/science/article/pii/S1570870505001149

[12] Eriksson G., Linder S., Wiklundh K., *ET AL.*: 'Urban peer-to-peer MIMO channel measurements and analysis at 300 MHz'. Proc. IEEE Milcom 2008, San Diego, CA, USA, November 2008

[13] Gudmundson M.: 'Correlation model for shadow fading in mobile radio systems', *Electron. Lett.*, 1991, **27**, (23), pp. 2145–2146

[14] Erceg V., Greenstein L.J., Tjandra S.Y., *ET AL.*: 'An empirically based path loss model for wireless channels in suburban environments', *IEEE J. Sel. Areas Commun.*, 1999, **17**, (7), pp. 1205–1211

[15] Pedersen K.I., Mogensen P.E., Fleury B.H.: 'A stochastic model of the temporal and azimuthal dispersion seen at the base station in outdoor propagation environments', *IEEE Trans. Veh. Technol.*, 2000, **49**, (2), pp. 437–447

[16] Cassioli D., Win M.Z., Molisch A.F.: 'The ultra-wide bandwidth indoor channel: From statistical model to simulation', *IEEE J. Sel. Areas Commun.*, 2002, **20**, (6), pp. 1247–1257
[17] Nilsson J., Sterner U.: 'Robust MPR-based flooding in mobile ad-hoc networks'. 2012–Milcom 2012 Military Communications Conf., 2012, pp. 1–6
[18] Ahlin L., Zander J.: 'Principles of wireless communications' (Studentlitteratur, Lund, 1998, 2nd edn.)
[19] Macker J.: 'Simplified multicast forwarding (SMF)'. IETF, Network Working Group, Internet-Draft, January 2012
[20] Clausen T., Jacquet P.: 'Optimized link state routing protocol (OLSR)'. IETF, Network Working Group, RFC 3626, October 2003

doi: 10.1049/joe.2014.0277